



Development of a Novel Super-active Ziegler-Natta Polyethylene Catalyst: Study on Structure, Performance and Application

M. A. Nikoohemmat^a, H. Mazaheri^{*a}, A. H. Joshaghani^a, E. Joudaki^b

^a Department of Chemical Engineering, Arak Branch, Islamic Azad University, Arak, Iran

^b Department of Chemical Engineering, Faculty of Engineering, Arak University, Arak, Iran

PAPER INFO

Paper history:

Received 11 July 2023

Received in revised form 28 August 2023

Accepted 16 September 2023

Keywords:

Polyethylene Pipes

Malvern

Super-active Catalyst-510

Ziegler-Natta Catalysts

ABSTRACT

In this research, the synthesis process of a novel super-active catalyst, named SAC-510 is investigated at experimental scale. The authors compared the analyzed data against those derived from a popular catalyst, *Finix-112*, and several other available alternatives. The data indicated that SAC-510 catalyst derived the optimal activity from its spherical particles. Titanium and other chemical elements were less uniformly distributed in SAC-510 than in *Finix-112* samples, with the mean particle size being slightly larger than that found in *Finix-112*. The pores' dispersion and sizes in SAC-510 were not as uniformly distributed as those in *Finix-112* catalyst. Lastly, both SAC-510 and *Finix-112* catalysts were equally adaptable for use in high-density polyethylene pipes (grade 100). Compared to other commercially available catalysts, the major advantages of SAC-510 are the economical use of hydrogen and monomers, and low purging of its valuable gases during the polymerization process. The results obtained are as follows: the increase in oxidative induction time efficiency with SAC catalyst compared to *Finix* catalyst by 5.8%, activity by 35.7%, hydrogen responsibility by 24.39%, 1-butene consumption by 8.38% and triethylaluminium consumption by 27.27%.

doi: 10.5829/ije.2024.37.01a.02

NOMENCLATURE

SAC-510	Super active catalyst	d	Diameter
PSD	Particle size distribution	DSC	Differential Scanning Calorimeter
OIT	Oxidation Induction Time	V_p	Pore volume
GPC	Gel permeation chromatography	r_p	Pore peak radius
HDPE	High density polyethylene	a_p	Specific pore area
PE100	Polyethylene pipe grade of 100	Greek Symbols	
SEM	Scanning electron microscopy	μ	Micron

1. INTRODUCTION

Society, in general, and the industry, in particular, have significantly included plastics for changing different materials. High density polyethylene (HDPE) is a semi-crystalline polymer widely used for the transport of drinking water supplies (1, 2). These are often exposed to different weathering conditions, for example in outdoor applications or when the freshly extruded pipes are stored in the open before their installation (3). Polyethylene (PE) is known as one of the most commonly-employed

thermoplastic polymer, which have demonstrated its brilliant advantages in different industrial-based activities like wires/cables insulation, agricultural mulch, membrane-based gas separation and medical engineering due to its ease of installation, absence of corrosion-related problems, low cost and projected 50 to 100-year service life (4-6). Ziegler-Natta catalyst is a commonly-used catalyst in a bimodal slurry system for HDPE production. This promising catalyst is made based on the mixture of different chemical components that are prominently applied in the synthesis process of 1-alkenes

*Corresponding Author Email: Hossein.Mazaheri@iau.ac.ir
(H. Mazaheri)

polymers (i.e., alpha-olefins) (7, 8). Titanium, and to a lesser extent, chrome and vanadium are regarded as important metallic elements in Ziegler-Natta catalysts (9). They have enabled scientists to polymerize many organic compounds, such as alkenes and dienes with superior activity and selectivity, under a wide variety of experimental conditions. Since their advent, these catalysts have also played a significant role in the development of valuable products, highly needed in petrochemical and plastic industries (9). In this context, the role of titanium and magnesium is particularly well known in the production and use of polyethylene products (10). Currently, scientists are conducting much research with a focus on the activity, particle morphology and distribution, hydrogen response, and performance of catalysts and co-catalysts (11-13).

Among the commonly-applied polymerization processes, ethylene slurry has attracted much scientific attention. In addition to improving the activity of catalysts, controlling the particle size and its distribution in polyethylene products are of significant importance (14-17). In the recent published research articles, various aspects of catalysts and their interactions with co-catalysts and intermediate metals have been investigated. These include, *a*) controlling titanium oxidation; *b*) effect of external and internal donors (18, 19); *c*) the role of co-catalysts (20); *d*) effect of newly developed catalysts (21, 22); and, *e*) synthetic and modelling studies in the polymerization field (23-26). In addition to the molecular structures of catalysts, the polymerization and industrial process have an essential role in the production of polymers with a variety of properties, and promoting scientific research on these products (27-30). During 1980's and 1990's, a series of patented methods on the preparation of new Ziegler-Natta catalysts has been introduced (31, 32). Later studies proposed and examined the role of titanium alkoxide to replace the use of Titanium tetrachloride (TiCl_4). In these products at least one alkoxide ligand connects Ti (OR)₄ to tetra-titanium alkoxide. A good example of this subject is the polymerization of olefin compounds (33-35).

To introduce a wide range of molecular weights in manufacturing resins, Ziegler-Natta catalysts require different reactors that operate under specific conditions of temperature, monomers, and hydrogen concentration, used in series or singly, which involve high costs (17, 36-38). In this context, there exists an urgent need for new catalysts with better performance to produce bimodal resins with added market value. For this purpose, two methods are popular for the preparation of the main components of the catalyst. The first method involves a solid carrier, consisting of a magnesium dihalide reaction with titanium or vanadium in a suspended hexane environment. This method provides the components of the catalyst, although it is difficult to control the polyethylene product, the particle size, and its

distribution (39). In the second method, a magnesium compound, such as magnesium dichloride, is dissolved in a solvent, so that homogeneous solid particles of magnesium or titanium precipitate after adding a titanium compound. This process can provide the main component of the catalyst upon its solid processing with another liquid titanium compound and a co-catalyst (40).

This study aims to synthesize and manufacture a novel and efficient super-active Ziegler-Natta catalyst, named *SAC-510* toward the production of a new generation of high-density polyethylene pipes. Subsequently, the authors analyzed the particle morphology and its performance, compared to a popular catalyst, *Finix-112*, and several other commercially available alternatives. We have obtained some promising results, which are presented and discussed in the present article.

2. MATERIALS AND METHODS

2. 1. Materials All of the materials for the polymerization processes of both the support catalyst, and the final super-active catalyst (SAC-510) were obtained from the Shazand Petrochemical Technology Company (Arak, Iran) and Pooyesh Co. (Tehran, Iran). Hexane (C_6H_{14}) was utilized as the solvent and copolymerization agent. Ethylene was used as the main feed for the polymerization process. Lastly, 1- butylene and hydrogen were used as the components required for the polymerization. Triethylaluminium (97%) was purchased from Fluka Chemie GmbH (Buchs, Switzerland). Oxygen 4.5 (purity 99.995%) and nitrogen 5.0 (99.999% purity) were obtained from the Shazand Petrochemical company.

2. 2. Equipment

2. 2. 1. Glove Box To store and preserve the catalysts and co-catalysts in this study, we used a glove box unit (Cleatech; Orange, CA, USA). This unit prevented the active sites in catalysts and sensitive chemicals from getting contaminated and oxidized, under a nitrogen atmosphere.

2. 2. 2. Scanning Electron Microscopy/ Energy Dispersive X-ray Analysis (SEM/EDX)

The surface morphology of the catalyst was examined by Scanning Electron Microscope (SEM) (model JSM-5910, JEOL Inc., Peabody, MA, USA) under high vacuum microprobe. This microscope provided scanned images, analyzed the X-ray emitted from the particles, and determined the accurate weight and percentage of the elements contained in the samples [40].

2. 2. 3. Malvern Analyzer In addition to the SEM analysis, the particle sizes and molecules contained in the

samples were also measured on a Malvern analyzer (Entegris; Dresden, Germany). The images obtained from this analyzer were based on the principle of dynamic light scattering.

2. 2. 4 Buchi Reactor Made of stainless steel with a volume of 1 liter is used for slurry polymerization. The volume of the reactor jacket is 300ml. Addition of catalyst and co-catalyst is by injection under pressure.

2. 2. 5. Gel Permeation Chromatography (GPC)

To analyze the different particle species of large molecular sizes, such as polymers, we measured the particle's molecular weights on a gel permeation chromatography unit (GPC-150-II+IR5; Cambridge Polymer Group, Inc.; Woburn, MA, USA) (41).

2. 2. 6. Differential Scanning Calorimeter (DSC)

The objective of the test is to represent the duration in time of the heat stabilizer until its deterioration through oxygen and heat. The period of time from the switching over to oxygen until the onset of the oxidation reaction (point of intersection of the basis line with the tangent) is referred to as the induction period (Oxidation Induction Time, OIT). A long induction period shows good stabilization and vice versa. The described test method is carried out in dependence on DIN EN728 and we used Differential Scanning Calorimeter unit (Mettler-Toledo DSC 822e.) (42).

2. 2. 7. Huber Circulator We utilized a Huber circulating bath (Ministat CC3 Huber UK; Derbyshire, UK) to control the temperature within the reactor's jacket, ranging from -50°C to $+350^{\circ}\text{C}$.

The required materials and laboratory steps to prepare the 4th generation of Ziegler-Natta super-active catalyst are shown in Flowchart 1:

2. 3. Methods

2. 3. 1. Preparation and Polymerization The methods for the polymerization processes, as established by earlier studies (39, 40, 43).

2. 3. 1. 1. Magnesium Ethoxide Powder This material was necessary to make the base product. The construction of super active Ziegler-Natta catalysts for ethylene polymerization requires substrates for the stability of the active centers of the catalyst. Metal halides and oxides have been proposed as suitable bases for catalysts, and in the meantime, magnesium ethoxide is very suitable for making the super active Ziegler-Natta catalyst. To prepare the super active catalyst base, commercial magnesium ethoxide ($\text{Mg}(\text{OC}_2\text{H}_5)$) is first prepared in pure form with the conditions presented in Table 1. The average particle diameter of the primary magnesium ethoxide powder is 500 microns, so that more

than 90% of the particles have a diameter in the range of 200 microns to 1200 microns. Titanium sits better on the substrate when the size of the primary powder particles is reduced and their distribution is uniform. Magnesium ethoxide with a diameter of about 500 microns forms a suspension in an inert saturated hydrocarbon after mechanical crushing by a jet mill to a size of about 8 microns using a Jet pulverizer (Jet Mills; Moorestown, NJ, USA). Table 1 presents aims to present different features of the magnesium ethoxide for the catalyst bed.

2. 3. 1. 2. Magnesium Ethoxide Suspension Gel

The magnesium ethoxide powder was then suspended in a neutral, aliphatic hydrocarbon until the mixture was ready to convert into gel. Ideal hydrocarbons for this purpose are butane, hexane, cyclohexane, heptane, isooctane, and several others including toluene and xylene. Also, hydrogenated oils devoid of oxygen and sulphur would be appropriate. About 200 grams of the sample is taken under N_2 atmosphere and injected into a 5-liter reactor containing two liters of hexane. Then carbon tetrachloride is added and after mixing (100rpm), the temperature of the reactor is increased to about 60 degrees, and this process is allowed to continue for 24 hours. In this case, the solvent penetrates into the crystal layers and causes the particles to take a gel-like shape. If the gelling process has progressed correctly, after stopping the mixer, it takes about 30 minutes for the particles to settle.

Injecting 7 ml of titanium tetrachloride into the gel produced at 80 degrees Celsius to place titanium on the gel bed.

2. 3. 1. 3. Catalyst Assisted Preactivation

The choice of co-catalyst has a great influence on the performance of titanium-based Ziegler Natta catalysts. Catalyst assistance affects activity, molecular weight and molecular weight distribution. By increasing the amount of catalyst aid, the activity of all active centers decreases to almost one level. In order to produce active sites, which Mr. Kissin divided into five types by fluorescent distribution, the catalyst must be placed in the vicinity of triethyl aluminum (TEA) for a certain period of time.

2. 3. 1. 4. Determination Of The Catalyst Content

A 10ml aliquot of the catalyst was removed from its container, using a syringe, and poured in a small glass dish with known weight. After the sample was cooled

TABLE 1. Strouhal number for different geometric cases

Magnesium Species	Percentage of Total Weight
Total magnesium content	21-22%
Total $\text{Mg}(\text{OH})_2$ & MgCO_3 contents	<1%
Total $\text{C}_2\text{H}_5\text{OH}$ content	<0.3%

down, the weight of the empty dish is deducted from the total weight of the dish containing the catalyst 10ml aliquot. The net weight of the catalyst sample varies depending on the solvents, such as hexane, used for the polymerization processes.

2.3.1.5. Polymerization Prior to this step, the reactor was purged by running nitrogen (≤ 0.1 bar) through it at 100°C for 60 minutes. Subsequently, the oil circulator pump of the reactor was set at 4500 rpm, and the temperature reset to 60°C. At this temperature, the reactor was cleared with ethylene gas three times at 3-bar pressure. Then, 500 ml hexane at 0.1 bar, and 400 mg/ml triethylaluminium (TEAL) were injected into the reactor and the agitator turned on at 200 rpm. The TEAL was mainly used for the purpose of removing contaminations from the solvent and activation of sites in the catalyst. After 30 minutes from the injection of TEAL, 1-butylene was injected to the reactor at a set amount, and allowed to mix with TEAL and the solvent for 15 minutes with the agitator set at 200rpm. During a 30-min pre-activation time, the concentration of catalyst diluted in hexane reached 2mg/ml.

After determining the reactor's pressure at optimal temperature, the catalyst was injected in the reactor under pressure. Next, the reactor's software program was set to reaction mode and the polymerization synthesis plots being printed. During this process, the reaction temperature was closely monitored at 83°C ($\pm 1^\circ\text{C}$) while ethylene was being injected into the reactor at 8 bar. The estimated time for the polymerization of ethylene with 1-butylene in the presence of the catalyst SAC-510 was approximately 180 minutes. At the completion of this final step, the reactor's software program was set to "Reaction Off". This terminated the ethylene entry into the reactor and the circulator's temperature was set at 60°C. After the reactor cooled down, the lid was opened, the chamber was cleaned thoroughly with nitrogen, and the catalyst and solvents residues were wiped out.

2.3.2. Surface Area Analysis (SSA) The surface area and pore size analysis of the catalyst were carried out by Surface Area Analyzer (Quanta chrome Nova Station A), using nitrogen adsorption method. The sample was initially degassed at 200 °C for 4 h. Surface area of the catalysts was calculated from the nitrogen adsorption isotherm data, using Brunauer, Emmett and Teller (BET) equation. The pore size and pore volume of the catalysts were calculated from N₂ adsorption isotherm data with the help of Barrett, Joyner, Halenda (BJH) model (44).

3. RESULTS AND DISCUSSION

3.1. Particles Morphology Understanding the

morphology of micro particles can assist us predict their mass transfer and heat as they go through polymerization processes (45). Initially, monomers penetrate into the catalyst's pores and start numerous active reaction sites, forming the basic polymer particles and clumps as they combine with the catalyst and continue to grow. Later, layers of the polymer are deposited on the catalyst's spherical macro particles, leading to the final polymerized product. Thus, examining the particles reflects the true physical nature of the combined polymer and catalyst (46). Results from this study's tests and experiments are presented below followed by the pertinent discussion under each subsection.

3.2. Energy Distribution Analyses of the Catalysts' Powders

Table 2 represents the results of energy distribution in the two powdered catalysts, *Finix-112* and *SAC-510*, under scanning X-ray analysis (SEM-EDXA). As shown in Table 2, four and three zones were examined, respectively, under SEM-EDXA using the powdered samples of *Finix-112* and *SAC-510* catalysts. The results indicated that there were relatively uniform percentages of the chemical elements, especially titanium, in the *Finix-112* samples. However, much less uniformity was observed in the *SAC-510* samples. Figure 1 shows the electron microscopic images of powdered *Finix-112* and *SAC-510* catalysts, and the differences in the distribution of the particles for both samples.

Evidently, the differences in the percentage and uniformity of the elemental distributions in both catalysts' samples arise from their chemical nature and formulation. Based on the images illustrated in Figure 1, it is perceived that the presence of smaller catalyst particles makes the mobility of larger particles easier, thereby facilitates the polymerization reaction. A major advantage of SEM-EDXA is its better capability of determining the compositional elements in powdered catalysts than that achieved by either XRF or ICP method. The SEM-EDXA method is able to recognize such elements as oxygen, carbon and halogen. Also, it

TABLE 2. Scanning electron microscopic features of the *Finix-112* and *SAC-510* powders

Finix-112	Ti	Mg	Cl	Al	O	Cu	Si
EDAX-1	4.94	20.98	35.85	0.49	37.32	0.42	-
EDAX-2	3.37	14.17	36.06	0.34	45.72	0.38	-
EDAX-3	3.79	15.7	39.28	0.36	40.60	0.28	-
EDAX-4	4.36	13.3	44.70	0.09	36.77	0.51	-
SAC-510	Ti	Mg	Cl	Al	O	Cu	Si
EDAX-1	8.01	14.45	42.36	1.82	30.99	1.47	0.89
EDAX-2	5.48	17.44	28.01	3.29	42.79	0.73	2.25
EDAX-3	6.25	18.51	32.21	3.4	35.64	0.76	2.24

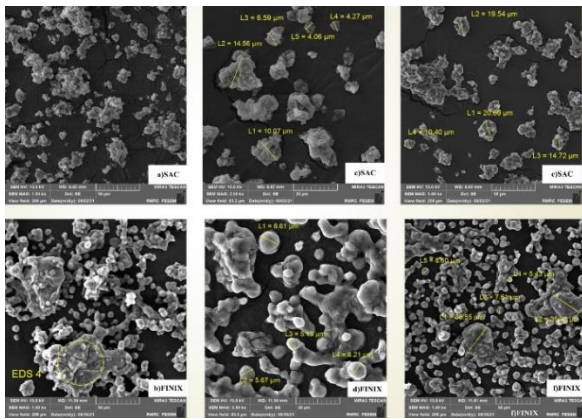


Figure 1. Scanning electron microscopic images of the catalysts Sac-510 and Finix-112 powders. a,b) SEM MAG=1 kx, 50µm; c,d) MAG=2.5kx, 20µm; e,f) SEM=1kx,50µm

provides the distribution patterns and variations in the concentration of elements in different areas of various samples at large magnification.

3. 2. Particle Size Distribution – Malvern’s Method

Figure 2 represents the particles’ volume of distribution and their sizes in the micron scale for both catalysts, based on Malvern’s method. As seen in Figure 2, the particles in both catalysts occurred similarly in one uniform population each (range: 2-11 µm vs 3-30 µm). The single peak (50%) for Finix-112 catalyst occurred approximately at 6.8µ while that of SAC-510 was about 8.6 µm. The data for the particle size distribution in both groups of catalysts are summarized in listed in Tables 3

and 4.

The data in Tables 3 and 4 indicate that the average particle size for SAC-510 catalyst was slightly larger than that of Finix-112. In this context, 10% of the SAC-510

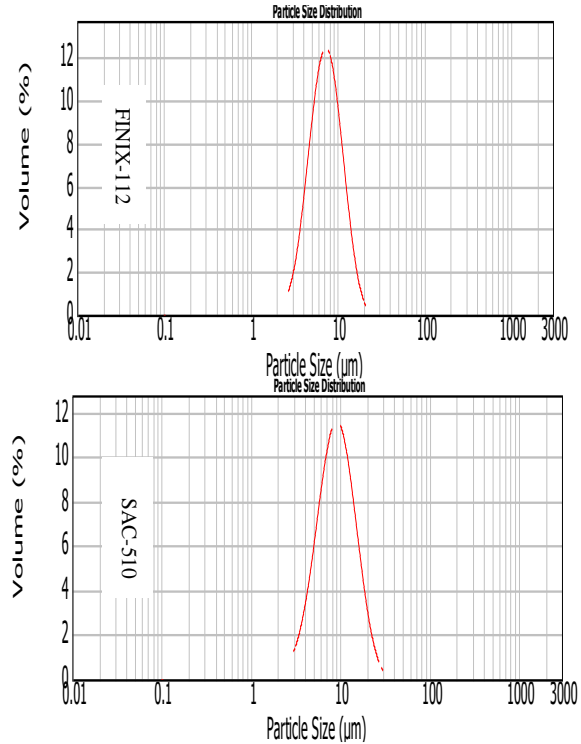


Figure 2. Particle size distribution of SAC-510 (super active) and Finix-112 catalysts

TABLE 3. Particle size distribution in Finix-112 and SAC-510 catalysts

	Size (µm)	Vol Under %	Size (µm)	Vol Under %	Size (µm)	Vol Under %	Size (µm)	Vol Under %	Size (µm)	Vol Under %	Size (µm)	Vol Under %
FINIX-112	2	8.97	16	97.77	45	100	128	100	345	100	850	100
	3	11.39	17	98.55	50	100	132	100	370	100	898	100
	4	17.81	18	99.09	52	100	142	100	385	100	950	100
	5	28.31	19	99.45	54.3	100	160	100	400	100	1000	100
	6	40.66	20.5	99.77	58.5	100	168	100	450	100	1125	100
	7	52.83	22.3	99.91	63	100	177	100	500	100	1250	100
	8	63.66	24	99.98	68	100	190	100	525	100	1325	100
	9	72.69	26	100	73	100	205	100	550	100	1400	100
	10	79.9	28	100	76.5	100	227	100	575	100	1500	100
	11	85.46	30.2	100	80	100	250	100	600	100	1600	100
	12	89.66	32	100	89	100	262	100	634	100	1740	100
	13	92.76	34.8	100	98.2	100	275	100	668	100	1880	100
	14	95.02	37	100	111	100	297	100	735	100		
	15	96.63	40.5	100	125	100	320	100	800	100		

	Size (μm)	Vol Under %	Size (μm)	Vol Under %	Size (μm)	Vol Under %	Size (μm)	Vol Under %	Size (μm)	Vol Under %	Size (μm)	Vol Under %
SAC-510	2	4	16	89.6	45	100	128	100	345	100	850	100
	3	6.25	17	91.8	50	100	132	100	370	100	898	100
	4	10.42	18	93.56	52	100	142	100	385	100	950	100
	5	17.19	19	94.97	54.3	100	160	100	400	100	1000	100
	6	25.86	20.5	96.56	58.5	100	168	100	450	100	1125	100
	7	35.38	22.3	97.86	63	100	177	100	500	100	1250	100
	8	44.87	24	98.66	68	100	190	100	525	100	1325	100
	9	53.76	26	99.26	73	100	205	100	550	100	1400	100
	10	61.72	28	99.6	76.5	100	227	100	575	100	1500	100
	11	68.64	30.2	99.82	80	100	250	100	600	100	1600	100
	12	74.53	32	99.91	89	100	262	100	634	100	1740	100
	13	79.46	34.8	99.97	98.2	100	275	100	668	100	1880	100
	14	83.54	37	99.99	111	100	297	100	735	100		
	15	86.89	40.5	100	125	100	320	100	800	100		

TABLE 4. Particle distribution in the catalysts based on Malvern method

Catalyst	SAC-510	Finix-112
D (0.1)	3.9 μm	2.5 μm
D (0.5)	8.6 μm	6.8 μm
D (0.9)	16.2 μm	12.1 μm

particles fell within 3.9 μm in size while the same percentage of Finix-112 particles had a 2.5 μm size. Further, about 90% of the particles in SAC-510 group had a size of 16.2 μm while those in Finix-112 group were about 12.1 μm in size.

The mechanical measurement of catalysts' particle size and their distribution are performed broadly in industries, which is a critical parameter for manufacturing numerous products. In this respect, Malvern is a highly accurate method for measuring particle sizes ranging from low nanometer to several millimeters.

3.3. BET Test Using the popular (BET) test (23), we analyzed the features and dimensions of the pores in both Finix-112 and SAC-510 catalysts. The data from this analysis are presented in Table 5.

TABLE 5. Results of the SAC-510 and Finix-112 powders based on BET test

Property	SAC-510	Finix-112
Specific area (m^2/g)	22.492	24.759
Total Pore volume (cm^3/g)	0.1746	0.1213
Average pore dimension (nm)	31.051	19.592

The overall results obtained from BET test revealed that the specific area for the pores in SAC-510 was 9% less than that of Finix-112. Also, the mean dimension and volume of the pores in SAC-510 catalyst were greater than those determined for Finix-112 catalyst.

Considering the above data, it can be argued that the dimensional features of the porosity in SAC-510, compared to those in Finix-112, decreases the ability of this catalyst to respond to physical forces. Also, it is likely that larger pores may be deeper in SAC-510 with smaller lateral surfaces, which further contribute to its lower tolerance against shocks, vibrations and other destructive forces.

3.4. Barrett-Joyner-Halenda Test Also, we used another popular test, Barrett-Joyner-Halenda (BJH), to determine the volume and distribution of pores in the catalysts (23). The data from our BJH test on both catalysts are presented in Table 6. Specifically, Table 6 reflects accurate information about three important variables for each of the two catalysts: a), the pore volume (V_p); b) the pore peak radius (r_p); and c) specific pore area (A_p). Figure 3 schematically presents the scatter diagram of pores and dimensions of super active SAC-510 and Finix-112 catalysts.

TABLE 6. Results of the SAC-510 and Finix-112 powders based on BJH test

Variable	Unit	Finix-112	SAC-510
Pore Volume (V_p)	Cm^3/g	0.1231	0.1762
Pore Peak Radius (R_p)	Nm	5.29	10.65
Specific Pore Area (A_p)	m^2/g	31.951	28.827

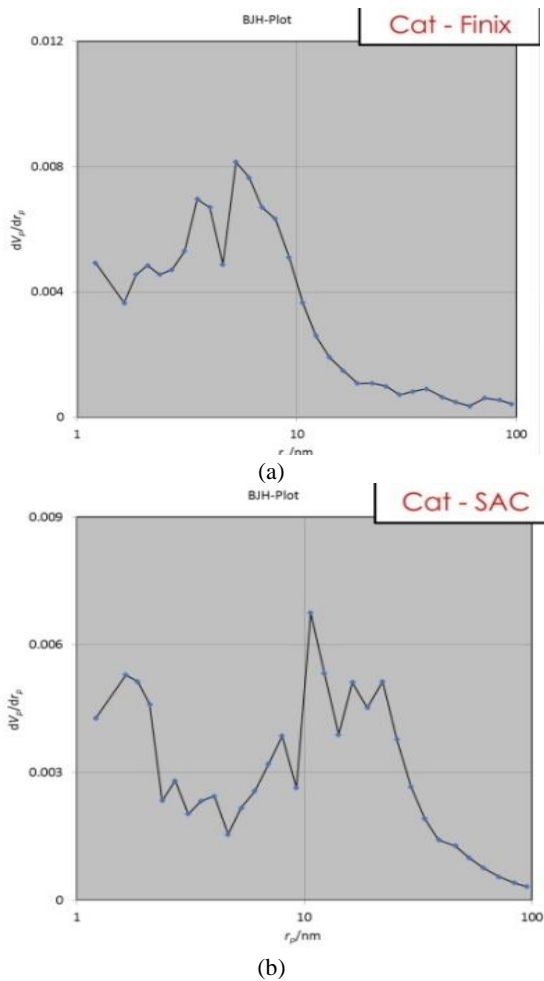


Figure 3. Scatter diagram of pores and dimensions of a) super active Finix-112 and b) SAC-510 catalysts. Key: V_p = Pore volume; R_p = Pore peak radius; a_p = Specific pore area

As seen in Table 6, the pore volume in catalyst SAC-510 was greater than that of Finix-112. This had an opposite effect on the specific surface and reduced this variable. Also as shown in Figure 3, the dV_p/dR_p ratios for SAC-510 indicate that the dispersion of the pores and sizes did not occur as uniformly as those found for Finix-112.

To assess the validity of the findings obtained through the BET analysis, we used BJH test (33). The advantage of BJH test is that it measures the volume and distribution of the pores while BET test provides a reliable measure of the areas associated with the solid material in the catalysts. Also, BJH test assists in obtaining approximate data regarding the absorption and release of isotherms, the pores' dimension, and their distribution within the catalysts.

3. 5. Gel Permeation Chromatography GPC-IR has been used to characterize the copolymer and the consequences are given in Figure 4 it is observed that the

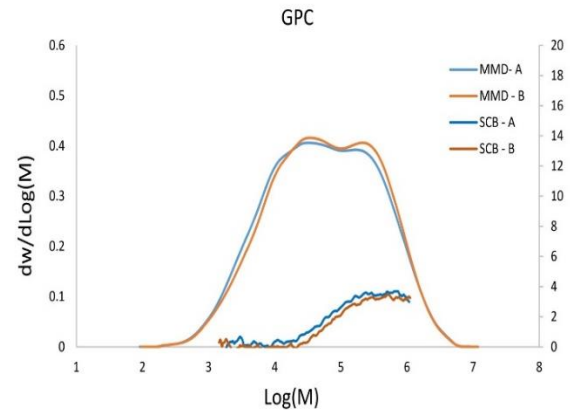


Figure 4. GPC analysis diagram of product HDPE-100 with novel and commercial catalyst A) HDPE-100 obtained from commercial catalyst (Finix112): B) HDPE-100 obtained from novel catalyst (SAC-510)

bimodal molecular weight has been formatted. The copolymer received from the novel catalyst has a high branch degree in the high molecular weight fraction and lower branch degree in the low molecular weight fraction, that's favorable to enhance the resin mechanical properties.

The polymer properties are determined by the characteristics of the polymer including molecular weight, its distribution, and degree of branching. The breath of the molecular weight distribution, M_w/M_n , additionally affects the process ability of the polymer. The degree of short chain branching strongly influences a few variables together with crystallinity and density, which in flip determines the last properties of the material. The slurry polymerization processes give resins, which have great mechanical properties preserving wonderful process ability. It can be found out via bimodal high molecular weight HDPE. The low molecular weight component product in a single reactor offers suitable process ability, even as the high molecular weight component created with inside the different reactor offers exceptional mechanical strength.

3. 6. Comparison of both SAC-510 and Finix-112 with Industrial Catalysts and Efficiency

Table 7 represents major important factors and performance about some currently used catalysts in chemical engineering science, as well as in industries, compared with the novel, super-active catalyst, SAC-510. All of the currently available catalysts have been used for the manufacturing of polyethylene pipes grade 100.

Hydrogen is the most broadly used chain-transfer agent for molecular weight control with Ziegler-Natta structures in industry. Hydrogen is the simplest commercially relevant chain-transfer agent in the low-pressure olefin polymerization process over the Ziegler-Natta catalysts.

Valuable and important points aspects that are suggested from the data analysis, as shown in Table 7 in support of the super-active SAC-510 catalyst application toward the manufacturing of grade 100 polyethylene pipes are as follows: a) superior performance and durability; b) little consumption of triethylaluminum, 1-Butylene and hydrogen; c) better hydrogen response; and, d) ideal strength of the polyethylene pipes made of HDPE-100 product compared to other currently available industrial catalysts.

As can be seen in Table 8, the efficiency with the Sack catalyst has a considerable advantage over other catalysts in almost all parameters, such as reducing 1-butene consumption, reducing hydrogen consumption, reducing triethylaluminum consumption and increasing activity, and using this Catalyst is recommended in the production of polyethylene 100 product.

3. 7. Oxidation Induction Time In Table 9, some characteristics of super catalyst product are listed with the products of other catalyst. The comparison of OIT in the product of the novel catalyst with the product of other catalyst shows an acceptable OIT and indicates the successful performance of the SAC-510 catalyst.

Oxidative induction time (OIT) is widely used for the determination of the thermal oxidative resistance of polyethylene materials. The OIT testing only provides a

relative measure of the level of antioxidants remaining in the pipe material but is a suitable analytical technique to monitor the degree of depletion of antioxidants from the pipe surface. Oxygen induction times (OIT) indicate the stabilities of the products (47). The concentration of effective antioxidant was assessed by determining the oxidation induction time (OIT) at 210 °C. The data presented on the deterioration of polyolefin pipes exposed to water containing chlorine dioxide have been mostly concerned with lifetime issues. Choosing a constant testing temperature which delivers OIT times of around 60 min for the unaged reference samples can be too high for the aged samples. On the other hand, a much lower temperature for OIT tests could result in high differences between the unaged and aged samples (48).

4. LIMITATIONS OF THE STUDY

This study faced several challenges due to limited or lack of laboratory equipment and organic chemicals when it was being conducted as follows:

1. Lack of nuclear magnetic resonance facility to quantify the extent that butylene-1 was incorporated into the copolymer chains at 125°C.
2. Difficulty with separating 1- butylene from the solvent due to their close boiling points.

TABLE 7. Results of the SAC-510 performance versus other industrial catalysts at our site (32)

Catalyst	Unit	PE100/article	PE100/THS	PE100/BCE7	PE100/Finix-112	PE100-/SAC510
1-Butene Consumption	Kg/ton PE	18.51	21.21	15.6	16.8	15.5
H ₂ Consumption	g/ton PE	1129.6	387	426	406	319
TEAL Consumption	Liter/ton PE	-	1.38	1.82	1.4	1.1
Q _{RA} H ₂ /C ₂ H ₄	-	8	3.5	7.5	4.1	3.3
Q _{RB} H ₂ /C ₂ H ₄	-	0	0.02	0.06-0.07	0.03	0.01
R _B Pressure	Bar gauge	2.5	3.5-4	2.5-3	2.6	2.8
Activity	Kg PE/g Catalyst	8.82	20.6	20.75	27	28
R _A Pressure	Bar gauge	-	-	-	-8.4	6.4

TABLE 8. Results of the SAC-510 efficiency versus other industrial catalysts at our site (32)

Catalyst	Unit	SAC/article	SAC /THS	SAC /BCE7	SAC /Finix-112
1-Butene Consumption	%	19.42%	36.83%	0.6%	8.38%
H ₂ Consumption	%	254.1%	21.31	33.54%	27.27%
TEAL Consumption	%	-	25.45%	67.27%	27.27%
Q _{RA} H ₂ /C ₂ H ₄	%	142.4%	6%	127.3%	24.39%
Q _{RB} H ₂ /C ₂ H ₄	%	0	100%	600%	200%
R _B Pressure	%	-10.7%	33.9%	-1.78%	-7.14%
Activity	%	68.5%	26.42%	25.89%	3.57%
R _A Pressure	%	-	-	-	31.25%

TABLE 9. Material properties of the reference samples (Mw: molecular weight, OIT: oxidation induction time at 210 °C, X: degree of crystallinity)

HDPE pipe	PE ₁ (48)	PE ₂ (48)	PE _{SAC-510}	PE _{Finix-112}
Molecular weight (M _w)	115561	131344	241203	233372
OIT (min)	66	67	69	65
Crystallinity (%)	52	45	51.22	49.92

3. Inability to conduct mechanical strength and strain tests on the PE-100 pipe made of the novel catalyst. Ideal tests would include burst, hydro, and slow-crack-growth tests.

5. RECOMMENDATIONS FOR FUTURE STUDIES

We recommend the conduction of future researches with a focus on the following points:

1. Adjusting the use of hydrogen to improve control over the catalyst's molecular mass.
2. Testing other co-catalysts and investigating their effects on the morphology and activity of the resultant catalyst.
3. Applying different organic solvents with higher boiling points to facilitate their removal from 1-butylene.
4. Rheological and viscosity experiments on the polymer's long chains at zero shear rate.

6. CONCLUSION

The prominent purpose of this research paper is the experimental production of a novel, cost-effective and efficient super-active catalyst (SAC-510) (patent pending), which is potentially ideal for manufacturing a wide range of high-density polyethylene pipes used in various industrial applications. The generation process of SAC-510 heterogeneous catalyst took place on a bed of magnesium ethoxide (as the co-catalyst), and halocarbon in the presence of titanium tetrachloride. The copolymerization of ethylene and 1-butylene slurry was implemented in a Buchi's reactor under optimal conditions of temperature and barometric pressure.

Based on the SEM results, it was corroborated that the SAC-510 catalyst derives its active property from its spherical particles, in the presence of triethylaluminium in Buchi's reactor. Analysis of the obtained results from BET test demonstrated that the specific area for the pores in SAC-510 was 9% less than that of Finix-112. Also, the particle distribution of SAC-510 catalyst was about 60% greater than that of determined for Finix-112 catalyst, which demonstrates the superior efficiency of SAC-510.

Compared to other catalysts, the major advantages of SAC-510 are: a) the economical use of hydrogen and comonomers, b) better crystalizing capacity, and, c) low purge of valuable gases during the polymerization process. Further improvements on this subject await future research.

7. ACKNOWLEDGEMENTS

The authors are thankful to the professors and staff of the Department of Chemical Engineering, Arak Branch, Islamic Azad University, Arak, Iran.

8. SUPPLEMENTAL DATA AVAILABILITY

The detailed datasets generated and analyzed during the current study are available for review from the Corresponding Author upon request.

9. REFERENCES

1. Devilliers C, Fayolle B, Laiarinandrasana L, Oberti S, Gaudichet-Maurin E. Kinetics of chlorine-induced polyethylene degradation in water pipes. *Polymer Degradation and Stability*. 2011;96(7):1361-8.
2. Abeysinghe S, Gunasekara C, Bandara C, Nguyen K, Dissanayake R, Mendis P. Engineering performance of concrete incorporated with recycled high-density polyethylene (HDPE)—A systematic review. *Polymers*. 2021;13(11):1885.
3. Maria R, Rode K, Brüll R, Dorbath F, Baudrit B, Bastian M, et al. Monitoring the influence of different weathering conditions on polyethylene pipes by IR-microscopy. *Polymer Degradation and Stability*. 2011;96(10):1901-10. 10.3233/JIFS-201201
4. Whelton AJ, Dietrich AM. Critical considerations for the accelerated ageing of high-density polyethylene potable water materials. *Polymer Degradation and Stability*. 2009;94(7):1163-75. <https://doi.org/10.1016/j.polymdegradstab.2009.03.013>
5. Ronca S. Polyethylene. *Brydson's plastics materials*: Elsevier; 2017. p. 247-78.
6. Zha S, Lan H-q, Huang H. Review on lifetime predictions of polyethylene pipes: Limitations and trends. *International Journal of Pressure Vessels and Piping*. 2022;198:104663. 10.1016/j.ijpvp.2022.104663
7. Soga K, Shiono T. Ziegler-Natta catalysts for olefin polymerizations. *Progress in Polymer Science*. 1997;22(7):1503-46. [https://doi.org/10.1016/S0079-6700\(97\)00003-8](https://doi.org/10.1016/S0079-6700(97)00003-8)
8. Zarupski J, Piovano A, Signorile M, Amodio A, Olivi L, Hendriksen C, et al. Silica-magnesium-titanium Ziegler-Natta catalysts. Part 1: Structure of the pre-catalyst at a molecular level. *Journal of Catalysis*. 2023;424:236-45. <https://doi.org/10.1016/j.jcat.2023.05.024>
9. Zifang G, Wei C, Junling Z, Hongxu Y. Novel high performance Ziegler-Natta catalyst for ethylene slurry polymerization. *Chinese Journal of Chemical Engineering*. 2009;17(3):530-4. 10.5829/IJE.2022.35.11B.15
10. Galli P, Luciani L, Cecchin G. Advances in the polymerization of polyolefins with coordination catalysts. *Die Angewandte*

- Makromolekulare Chemie: Applied Macromolecular Chemistry and Physics. 1981;94(1):63-89.
11. Böhm LL, editor High mileage Ziegler-catalysts: excellent tools for polyethylene production. *Macromolecular Symposia*; 2001: Wiley Online Library.
 12. Klaue A, Kruck M, Friederichs N, Bertola F, Wu H, Morbidelli M. Insight into the synthesis process of an industrial Ziegler–Natta catalyst. *Industrial & Engineering Chemistry Research*. 2018;58(2):886-96. 10.1021/acs.iecr.8b05296
 13. Qian A, Han X, Liu Q, Ye L, Pu X, Chen Y, et al. Ultrathin Pd metallenes as novel co-catalysts for efficient photocatalytic hydrogen production. *Applied Surface Science*. 2023;618:156597.
 14. Klaue A, Kruck M, Binell P, Friederichs N, Bertola F, Wu H, et al. Ziegler–Natta catalyst sonofragmentation for controlling size and size distribution of the produced polymer particles. *AIChE Journal*. 2019;65(9):e16676. <https://doi.org/10.1002/aic.16676>
 15. Ikeda T, Wada T, Bando Y, Chammingkwan P, Taniike T. Bottom-Up Synthesis of Multi-Grained Ziegler–Natta Catalyst Based on MgO/MgCl₂/TiCl₄ Core–Shell Catalyst. *Catalysts*. 2021;11(9):1092.
 16. Yashiki T, Minami S. Solid titanium catalyst component, ethylene polymerization catalyst containing the same, and ethylene polymerization process. Google Patents; 2004.
 17. Zeynali M, Ranjbarbarano H, Olad A. Study of Titanium/Vanadium Ziegler–Natta hybrid catalysts performance in slurry-phase ethylene polymerization for producing polyethylene with broad/bimodal molecular weight distribution. *Journal of Polymer Research*. 2023;30(3):100.
 18. Vyas PB, Kaur S, Patil HR, Gupta VK. Synthesis of polypropylene with varied microstructure and molecular weights characteristics using supported titanium catalyst system. *Journal of polymer research*. 2011;18(2):235-9. 10.1007/s10965-010-9411-7
 19. Gao F, Xia X, Mao B. MgCl₂-supported catalyst containing mixed internal donors for propylene polymerization. *Journal of Applied Polymer Science*. 2011;120(1):36-42. 10.1002/app.31363
 20. Zhang HX, Lee YJ, Park JR, Lee DH, Yoon KB. Control of molecular weight distribution for polypropylene obtained by a commercial Ziegler–Natta catalyst: effect of a cocatalyst and hydrogen. *Journal of Applied Polymer Science*. 2011;120(1):101-8. 10.1007/s00289-011-0472-5
 21. Marchetti F, Pampaloni G, Patil Y, Galletti AMR, Renili F, Zacchini S. Ethylene polymerization by niobium (V) N, N-dialkylcarbamates activated with aluminum co-catalysts. *Organometallics*. 2011;30(6):1682-8. <https://doi.org/10.1021/ja00823a064>
 22. Thorne JE, Zhao Y, He D, Fan S, Vanka S, Mi Z, et al. Understanding the role of co-catalysts on silicon photocathodes using intensity modulated photocurrent spectroscopy. *Physical Chemistry Chemical Physics*. 2017;19(43):29653-9. <https://doi.org/10.1021/acsenergylett.9b02555>
 23. Machado F, Lima EL, Pinto JC, McKenna TF. An experimental study on the early stages of gas-phase olefin polymerizations using supported Ziegler–Natta and metallocene catalysts. *Polymer Engineering & Science*. 2011;51(2):302-10. <https://doi.org/10.1002/pen.21830>
 24. Alshaiban A, Soares JB. Mathematical Modeling of the Microstructure of Poly (propylene) Made with Ziegler-Natta Catalysts in the Presence of Electron Donors. *Macromolecular Reaction Engineering*. 2011;5(2):96-116. <https://doi.org/10.1002/mren.201000036>
 25. Yan W-C, Dong T, Zhou Y-N, Luo Z-H. Computational modeling toward full chain of polypropylene production: From molecular to industrial scale. *Chemical Engineering Science*. 2023;269:118448. <https://doi.org/10.1016/j.ces.2023.118448>
 26. Jung K, Corrigan N, Wong EH, Boyer C. Bioactive synthetic polymers. *Advanced Materials*. 2022;34(2):2105063. <https://doi.org/10.1002/adma.202105063>
 27. Cho HS, Choi YH, Lee WY. Characteristics of ethylene polymerization over Ziegler–Natta/metallocene catalysts: Comparison between hybrid and mixed catalysts. *Catalysis today*. 2000;63(2-4):523-30. [https://doi.org/10.1016/S0920-5861\(00\)00499-5](https://doi.org/10.1016/S0920-5861(00)00499-5)
 28. Liu B, Fukuda K, Nakatani H, Nishiyama I, Yamahiro M, Terano M. 27Al MAS solid state NMR study on coordinative nature of alkyl-Al cocatalysts on a novel SiO₂-supported Ziegler–Natta catalyst for controlled multiplicity of molecular weight distribution. *Journal of Molecular Catalysis A: Chemical*. 2004;219(2):363-70. <https://doi.org/10.1021/ja01510a019>
 29. Alizadeh M, Mostoufi N, Pourmahdian S, Sotudeh-Gharebagh R. Modeling of fluidized bed reactor of ethylene polymerization. *Chemical Engineering Journal*. 2004;97(1):27-35. 10.1016/S1385-8947(03)00133-5
 30. Fukuda K, Liu B, Nakatani H, Nishiyama I, Yamahiro M, Terano M. Significant variation of molecular weight distribution (MWD) of polyethylene induced by different alkyl-Al co-catalysts using a novel surface functionalized SiO₂-supported Ziegler-Natta catalyst. *Catalysis Communications*. 2003;4(12):657-62. <https://doi.org/10.1016/j.catcom.2003.10.001>
 31. Berthold J, Diedrich B, Franke R, Hartlapp J, Schafer W, Strobel W. Process for the preparation of a polyolefin, and a catalyst for this process. Google Patents; 1984.
 32. J.C Bailly, S. Sandis, inventors; BP Chemicals Ltd. Ziegler-Natta catalyst. United States patent US 4,960,741,1990.
 33. Mao B, Yang A, Zheng Y, Yang J, Li Z. Catalyst system for use in olefinic polymerization. Google Patents; 1988.
 34. Razavi-Nouri M. Studies of comonomer distributions and molecular segregations in metallocene-prepared polyethylenes by DSC. *Polymer testing*. 2006;25(8):1052-8. <https://doi.org/10.1016/j.polymertesting.2006.07.004>
 35. Vadlamudi M, Subramanian G, Shanbhag S, Alamo R, Varma-Nair M, Fiscus D, et al., editors. *Molecular Weight and Branching Distribution of a High Performance Metallocene Ethylene 1-Hexene Copolymer Film-Grade Resin*. *Macromolecular symposia*; 2009: Wiley Online Library.
 36. Fazeli N, Arabi H, Bolandi S. Effect of branching characteristics of ethylene/1-butene copolymers on melt flow index. *Polymer testing*. 2006;25(1):28-33. 10.1016/j.polymertesting.2005.09.008
 37. Keating M, Lee I-H, Wong CS. Thermal fractionation of ethylene polymers in packaging applications. *Thermochimica acta*. 1996;284(1):47-56. <https://doi.org/10.1021/acs.macromol.2c00773>
 38. Mohammadi Z, Moradi G, Teimoury H. Ziegler Natta catalyst by precipitation of soluble precursor in different synthesis conditions. *Journal of Organometallic Chemistry*. 2023;991:122675. 10.1016/j.jorganchem.2023.122675
 39. Monji M, Pourmahdian S, Vatankhah M, Taromi FA. Synthesis of highly improved Ziegler-Natta catalyst. *Journal of applied polymer science*. 2009;112(6):3663-8. <https://doi.org/10.1002/app.29786>
 40. Nowlin TE, Mink RI, Kissin YV. Supported Magnesium/Titanium-Based Ziegler Catalysts for Production of Polyethylene. *Handbook of Transition Metal Polymerization Catalysts*. 2010;131. 10.5829/IJE.2023.36.04A.02
 41. Nikoohemmat MA, Mazaheri H, Joshaghani A, Joudaki E. Investigation on Physical and Mechanical Properties of High Density Polyethylene (PE100) Using Novel Catalyst. *International Journal of Engineering, Transactions B:*

- Applications. 2022;35(11):2205-12. 10.5829/IJE.2022.35.11B.15
42. Shariatzadeh S, Salimi M, Fathinejad H, Hassani Joshaghani A. Nanostructured α -Fe₂O₃: Solvothermal synthesis, characterization, and effect of synthesis parameters on structural properties. International Journal of Engineering, Transactions C: Aspects. 2022;35(6):1186-92. 10.5829/IJE.2022.35.06C.10
43. ASTM D. 1505-10-Standard Test Method for Density of Plastics by the Density-Gradient Technique. Current Edition Approved Jul. 2010;1:7.
44. Karevan M. Investigation of Carbon Black/Polyester Micro-composites: An Insight into Nano-size Interfacial Interactions. International Journal of Engineering, Transactions C: Aspects 2022;35(6):1135-43. 10.5829/IJE.2022.35.06C.05
45. Kissin YV, Mink R, Nowlin T. Ethylene polymerization reactions with Ziegler-Natta catalysts. I. Ethylene polymerization kinetics and kinetic mechanism. Journal of Polymer Science Part A: Polymer Chemistry. 1999;37(23):4255-72.
46. McKenna T, Dupuy J, Spitz R. Modeling of transfer phenomena on heterogeneous Ziegler catalysts. III. Modeling of intraparticle mass transfer resistance. Journal of applied polymer science. 1997;63(3):315-22. [https://doi.org/10.1002/\(SICI\)10974628\(19970118\)63:3<315::AID-APP6>3.0.CO;2-Q](https://doi.org/10.1002/(SICI)10974628(19970118)63:3<315::AID-APP6>3.0.CO;2-Q)
47. Yu W, Azhdar B, Andersson D, Reitberger T, Hassinen J, Hjertberg T, et al. Deterioration of polyethylene pipes exposed to water containing chlorine dioxide. Polymer degradation and stability. 2011;96(5):790-7. <https://doi.org/10.1016/j.polyimdegradstab.2011.02.009>
48. Bredács M, Frank A, Bastero A, Stolarz A, Pinter G. Accelerated aging of polyethylene pipe grades in aqueous chlorine dioxide at constant concentration. Polymer Degradation and Stability. 2018;157:80-9. <https://doi.org/10.1016/j.polyimdegradstab.2018.09.019>

COPYRIGHTS

©2024 The author(s). This is an open access article distributed under the terms of the Creative Commons Attribution (CC BY 4.0), which permits unrestricted use, distribution, and reproduction in any medium, as long as the original authors and source are cited. No permission is required from the authors or the publishers.



Persian Abstract

چکیده

در این تحقیق، فرآیند سنتز یک کاتالیزور فوق فعال جدید به نام SAC-510 در مقیاس تجربی بررسی شده است. نویسندگان داده های تجزیه و تحلیل شده را با داده های به دست آمده از یک کاتالیزور پرکاربرد، Finix-112، و چندین جایگزین موجود دیگر مقایسه کردند. داده ها نشان داد که کاتالیزور SAC-510 فعالیت بهینه را از ذرات کروی خود به دست آورده است. تیتانیوم و سایر عناصر شیمیایی در SAC-510 با یکنواختی کمتری نسبت به نمونه های Finix-112 توزیع شده بودند، و اندازه متوسط ذرات در آن ها کمی بزرگتر از اندازه موجود در Finix-112 بود. پراکندگی و اندازه منافذ در SAC-510 به اندازه موارد موجود در کاتالیزور Finix-112 به طور یکنواخت توزیع نشده است. در نهایت، هر دو کاتالیزور SAC-510 و Finix-112 به یک اندازه برای استفاده در لوله های پلی اتیلن با چگالی بالا (درجه ۱۰۰) سازگار بودند. در مقایسه با سایر کاتالیزورهای تجاری موجود، مزایای عمده SAC-510 استفاده اقتصادی از هیدروژن و مونومرها و پاکسازی کم گازهای ارزشمند آن در طول فرآیند پلیمریزاسیون است. نتایج به دست آمده به شرح زیر است: افزایش راندمان زمان القای اکسیداتیو با کاتالیزور SAC-510 نسبت به کاتالیزور Finix-112 به میزان ۵۸ درصد، افزایش فعالیت به میزان ۳۵.۷ درصد، پاسخ دهی هیدروژن به میزان ۲۴.۳۹ درصد، کاهش مصرف ۱-بوتن به میزان ۸.۳۸ درصد و نیز کاهش مصرف تری اتیل آلومینیوم به میزان ۲۷.۲۷ درصد.